Editor : Advanced techniques on control & signal processing

Preprint · February 2020

DOI: 10.13140/RG.2.2.23483.57121

3 authors:

Hacene Mellah
Université de Bouira

Kamel Eddine Hemsas
Ferhat Abbas University of Setif

Taleb Rachid
Hassiba Benbouali University of Chlef

-PET- Vol. 57

ISSN : 1737-9934

Advanced techniques on control & signal processing

Proceedings of

Engineering & Technology

-PET-

Editor :

Dr. Ahmed Rhif (Tunisia)

International Centre for Innovation & Development

-ICID-

ISSN: 1737-9334
-PET- Vol. 57

ICID

International Centre for Innovation & Development

Proceedings of Engineering & Technology
-PET-

Advanced techniques on control & signal processing

Editor:

Dr. Ahmed Rhif (Tunisia)

International Centre for Innovation & Development

–ICID–

Summary

Simulation of the Stator and Rotor Winding Temperature of the Induction Machine for Continuous Service -Service Type S1 - Operation for Different Frequency

Hacene MELLAH[#1], Kamel Eddine HEMSAS[*2], Rachid TALEB[#3]

[#]*Department of Electrical Engineering, LGEER Laboratory, Faculty of Technology, University of Chlef, Algeria*
[*]*Department of Electrical Engineering, LAS Laboratory, Faculty of Technology, Ferhat Abbas Sétif 1 University, Algeria*

[1]has.mel@gmail.com
[2]hemsas.kamel@gmail.com
[3]ras.taleb@gmail.com

Abstract— **The temperature of electrical machines is one of the main factors limiting their performance. This temperature must respect the limits imposed by design and must not exceed them. Therefore, in order to be able to predict the temperature rise in the machines, thermal models are used. These allow on the one hand to thermally modeling the machines for monitoring, on the other hand to improve their design. This model must respect the complexity of the thermal phenomena by being able to take into account certain modifications on the design. This model must also consider the types of service of the machine, whether continuous, intermittent, and temporary or other types of service. In this paper, we deal with simulation of service type s1 - continuous service for different frequency of an induction motor. The main goal of this study is to prove the influence of the constant losses depend to the frequency to the stator and rotor winding temperature, the simulation results demonstrate to effect of the frequency to the temperature.**

Keywords— **Thermal Model, Winding Temperature, Induction Motor**

I. INTRODUCTION

Nowadays, the asynchronous machine is used more and more in the industrial domain. Indeed, appreciated for its standardization, its great robustness and its low costs of purchase and maintenance. For several years, we have noticed the widening of the scientific and manufacturer works concerning the drive of these machines [1]. The research of the electromechanical devices more and more flexible supported the appearance of the new particularly powerful systems. These systems generally rest on the association of an electronic device, allowing the control of the global system, and a rotating machine ensuring electromechanical conversion [1-3]. However, the increase in the specific powers and the use of novel control modes induce the harmonics of time [2] with frequencies beyond the audible aria, even with square wave voltages [1], the adaptation of the machines to these new applications generates an important internal heating. A rigorous study of the thermal behaviour of the electric machines is increasingly necessary [2]. Many authors describe the use of sensor as solution to the thermal problems of the induction machine [3] like infrared sensor [4, 5], thermocouple [5-9]. On the other hand, the infrared sensor gives a surface temperature measurement so the measurement is not accurate [3], and the thermocouple can require some machining for a correct placement, but it has the merit to be able to provide internal temperatures in exiguous places of the machine [3]. The problem of obtaining the rotors thermal information gene the sensor measurement procedure to be successful, however some solutions in the specialized literature can be cited, an optical link between the stator and the rotor proposed in [5-12]. Michalski et all in [5] propose an industrial rotary transformer, using a rings and brushes, a high frequency or infrared modules, all these methods are discussed in [3]. Some authors to avoid the problems of temperature measurement in electrical machines; proposes the use of the estimator and observer as Kalman [13-15], Luenberger [16] or based on artificial neural network [17, 18].

Zhao *et al* in [19] proposes an online rotor temperature estimation method of induction machine based on the noninvasive measurements of current and potential sensors.

Moreno et al. study the effect of frequency on the stator and rotor winding temperature but with their model [20]. In this paper, we use the model created by Al-Tayie et all in [15] to illustrate these effects.

II. LOSS IN ELECTRICAL MACHINES

Many authors [21-23] deal with the electrical machines loss model and their dependence on frequency and temperature.

Dong *et al.* in initial study use the time-step FEM to compute the winding ac losses in the end and slot winding at different speeds as represented in Fig. 1 [21]. In fact, the additional loss at ac input in the slot winding increases with frequency much faster than that in the end-winding, according to the amplification effect of the core on the leakage magnetic field, to simplify the study assume that the conductors are uniformly distributed in the slot.

ISSN 1737-9334

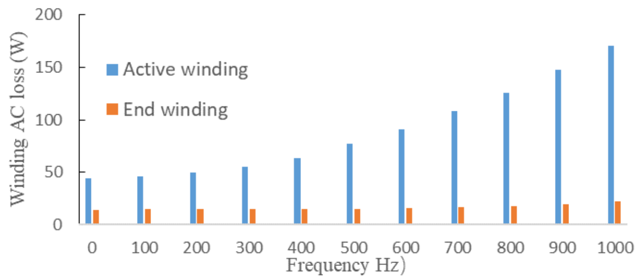

Fig. 1 Winding loss at different frequencies. Current amplitude: Im=6Arms [21].

Dong *et al.* [21] propose a fast and accurate analytical model to compute iron loss of inverter-fed induction machine, the advantage of this approach is able to takes account of the influence of the output voltage harmonics from the inverter on the iron loss of the motor based on the piecewise variable coefficients method. In addition, the proposed method incorporates slot harmonic component's influence on iron loss [21].

Xue *et al.* [22] study and proves by experiment that both the hysteresis and eddy current losses of non-oriented Si-steel laminations is a dependent on temperature.

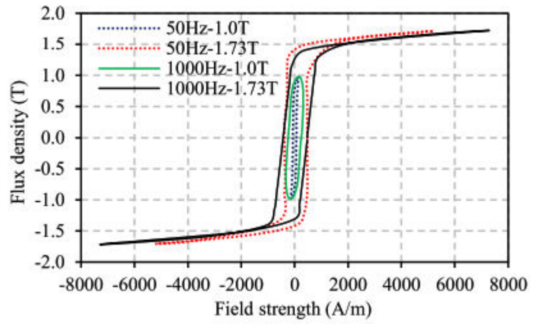

Fig. 2 Measured B–H loops at 40 °C when frequency is 50 and 1000 Hz [22]

Fig. 2 shows the measured B–H loops at 40 °C for two value of frequency 50 and 1000 Hz. We can see clearly that the B–H curves is distorted when the flux density is high due to the saturation at both 50 and 1000 Hz. The shape of B–H curves, which represents the iron losses in a time period, is frequency and flux density dependent [22].

Fig. 3 shows the comparison of the predicted iron loss by the model with the measured iron loss at different lamination temperatures. The modeled is able to accurately predict the iron loss at different flux densities and different frequencies when the lamination temperature remains 40 °C. However, the iron loss could vary significantly when the temperature increases from 40 °C to 100 °C, as shown in Fig. 3. However, the predicted iron loss cannot reflect this variation. Therefore, the prediction accuracies of this existing model can be significantly degraded when the temperature changes. The measured iron loss results show that both the hysteresis and eddy current losses vary linearly with temperature between 40 °C to 100 °C, a typical temperature range of electrical machines [23].

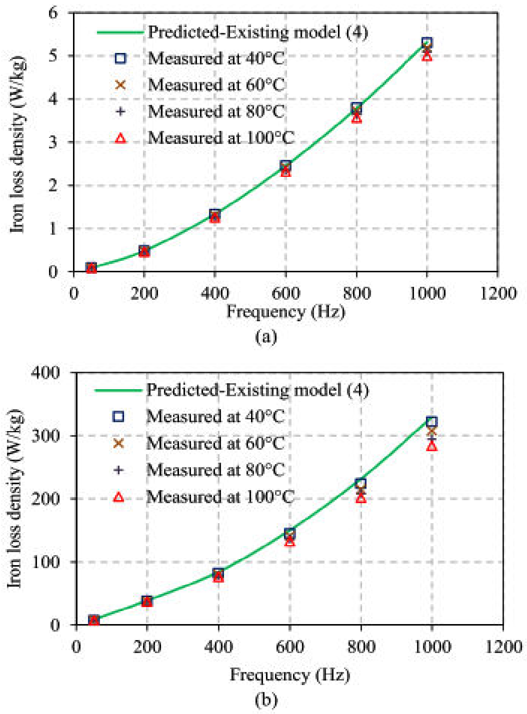

Fig. 3 Measured iron loss and predicted iron loss of existing model (4). (a) Bm =0.2 T. (b) Bm=1.73 T [23].

Xue *et al.* in [23] interested on the iron loss prediction for electrical machines fed by low switching frequency inverter, as results he summarize here results that the PWM influence on the iron loss on the electrical machines can be significantly increase, especially when the switching frequency is low.

III. A REVIEW OF THERMAL MOLDING METHODS

In the specialized literature, we find several thermal model of induction motors; we can summarize this model by three types.

A. *Simple Modeling*

We find many simple approaches in the literature in order to give bonds between the stator temperature and the rotor temperature. Beguenane *et al.* [24, 25] propose a model based on the electrical rotor resistance identification, which is unfortunately unable to identify the stator resistance; however, these articles propose two thermal approaches to bind two resistances of the electric model:

(1) The first method based on the EDF (Électricité De France) experiment. It considers that the rotor has a temperature higher of 10 °C than that the stator temperature;

(2) The second method based on work of Kubota [26]. It gives a simple relation of proportionality between two resistances calibrated on the face values of the maker badge. We find the proportionality method in other paper like [27]. On the other hand, later works were realized on EDF model

ISSN 1737-9334

and put a flat as for its validity for all the operating processes, especially NEMA design D machines with 8-13% slip [28].

B. Fine Modelling

It is based on the use of the finite element method with a detailed model geometric and mechanics. This makes it possible to obtain a complete cartography of the machine temperatures (Fig. 4). These results are very interesting since they make it possible to give an idea of the places where the temperature becomes critical according to the operations and answer the problems of the hot points [2, 3, 12].

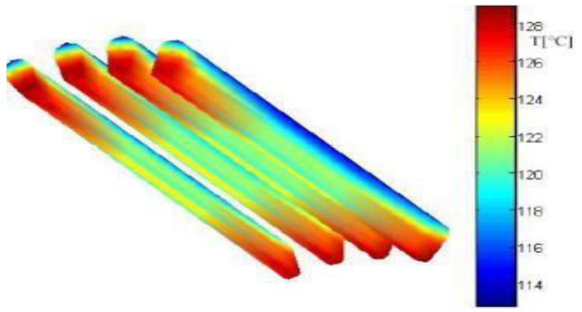

(a). Steady state stator winding temperature

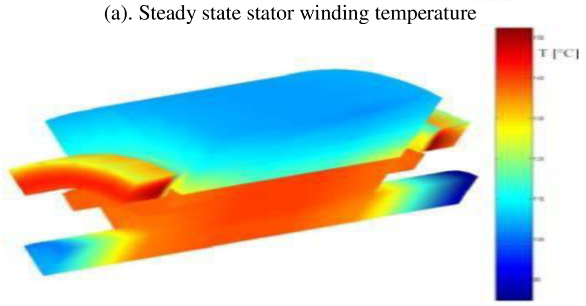

(b) Thermal cartography portion

Fig. 4 Thermal cartography portion of an induction machine, obtained by finite elements [12].

C. Electrical Equivalent Supply Networks (NODAL Method)

Those generally model the whole of the machine with nodes of temperature associated each material and divides the machine homogeneous region [26, 27]. The identification of this model is thus carried out either by finite elements, or by a great number of points of temperature measurement within the machine. These models are generally very detailed (Fig. 5) and thus too complex for our application in real time [26].

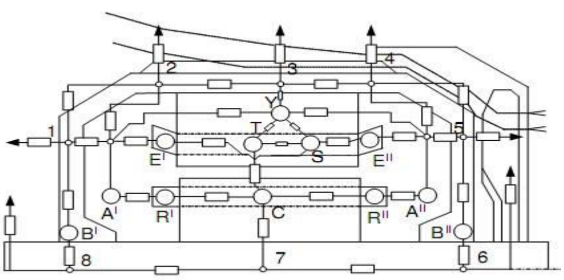

Fig. 5 Equivalent thermal models of the induction machine [4].

D. Simplified Models

Other researchers sought to simplify the models by gathering the losses in subsets and by approximating the temperature in an unspecified point with a simple exponential answer that one can simply represent by a resistance and a heat capacity (Fig. 6) [7, 17].

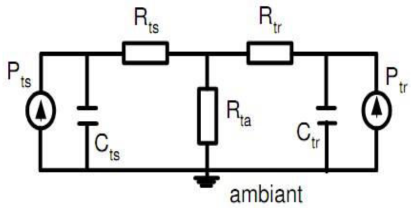

Fig. 6 Thermal model of the induction machine [7].

IV. THERMAL MODEL OF INDUCTION MOTOR

A variable-state model of the induction motor is required for the EKF algorithm. The twin-axis stator reference frame [15] is used to model the motor's electrical behavior, because physical measurements are made in this reference frame; the well-known linear relationship between resistance and temperature must be taken into account for the stator and rotor resistance.

$$\begin{aligned} R_s(\theta_s) &= R_{s0}(1+\alpha_s\theta_s) \\ R_r(\theta_r) &= R_{r0}(1+\alpha_r\theta_r) \end{aligned} \tag{1}$$

Where: R_{s0}, R_{r0} stator and rotor resistance at the ambient temperature, $\boldsymbol{\alpha}_s$ and $\boldsymbol{\alpha}_r$ their thermal coefficients. In the electrical equation of IM model, we replace the fixed resistance Rs and R_r by an adaptive resistance Rs(θs) and Rr(θr), the electrical model is as fellow [15]:

$$\begin{aligned} \delta\frac{di_{ds}}{dt} &= -R_s(\theta_s)L_2\, i_{ds} + L_m^2\,\omega_r\, i_{qs} + R_r(\theta_r)\,L_m\, i_{dr} \\ &\quad + L_2\,L_m\,\omega_r\, i_{qr} + L_2\,V_{ds} \end{aligned} \tag{2}$$

$$\begin{aligned} \delta\frac{di_{qs}}{dt} &= -L_m^2\omega_r\, i_{ds} - R_s(\theta_s)L_2\, i_{qs} - L_2L_m\omega_r\, i_{dr} \\ &\quad + R_r(\theta_r)L_m\omega_r\, i_{qr} + L_2V_{qs} \end{aligned} \tag{3}$$

$$\begin{aligned} \delta\frac{di_{dr}}{dt} &= R_s(\theta_s)L_m\, i_{ds} - L_1L_m\,\omega_r\, i_{qs} \\ &\quad - R_r(\theta_r)L_1 i_{dr} - L_1\,L_2\,\omega_r\, i_{qr} + L_2V_{qs} \end{aligned} \tag{4}$$

$$\begin{aligned} \delta\frac{di_{qr}}{dt} &= -L_1L_m\omega_r\, i_{ds} - R_s(\theta_s)L_2\, i_{qs} \\ &\quad - L_1L_2\omega_r\, i_{dr} + R_r(\theta_r)L_1\, i_{qr} + L_m\,V_{qs} \end{aligned} \tag{5}$$

Where: $\delta = L_1L_2 - L_m^2$, L_1 and L_2 stator and rotor self-inductances.

The mechanical behavior is as fellow:

$$T = b\,\omega_r + j\,p\,\omega_r + T_L \tag{6}$$

ISSN 1737-9334

However, the electromagnetic torque T can represented as a function of the stator and rotor current:

$$T = pL_m(i_{qs}i_{dr} - i_{ds}i_{qr}) \tag{7}$$

By equality of these two preceding equations, the speed equation is:

$$\frac{d\omega_r}{dt} = \frac{pL_m}{j}(i_{qs}i_{dr} - i_{ds}i_{qr}) - \frac{b}{j}\omega_r + \frac{T_L}{j} \tag{8}$$

The thermal model is derived by considering the power dissipation, heat transfer and rate of temperature rise in the stator and rotor. The stator power losses include contributions from copper losses and frequency- dependent iron losses [15].

$$pL_s = (i_{qs}i_{dr} - i_{ds}i_{qr})R_s(\theta_s) + k_{ir}\omega_r \tag{9}$$

Where: k_{ir} is it constant of iron loss. The rotor power losses are dominated by the copper loss contribution if the motor is operated at a low value of slip so:

$$pL_r = (i_{dr}^2 - i_{qr}^2)R_r(\theta_r) \tag{10}$$

Where: H_s, H_r are the stator and the rotor heat capacity respectively. A simple representation of the assumed heat flow is given in Fig. 7.

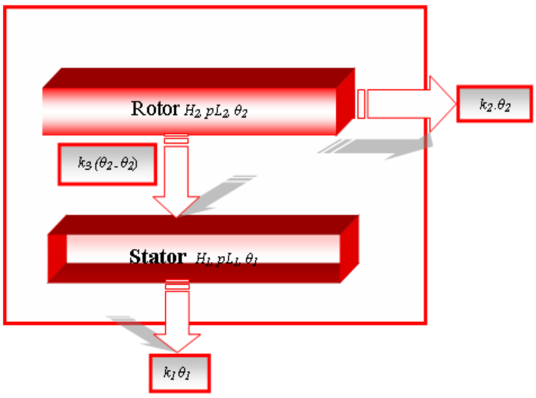

Fig. 7 Thermal model structure

Heat flow from the rotor is either directly to the cooling air with heat transfer coefficient k_2, or across the air gap to the stator with heat transfer coefficient k_3 [15].

$$pL_r = k_2\theta_r + H_r p\theta_r + k_3(\theta_r - \theta_s) \tag{11}$$

Heat flow from the stator is directly to the cooling air, with heat transfer coefficient k1[15]:

$$pL_s = k_1\theta_s + H_s p\theta_s - k_3(\theta_r - \theta_s) \tag{12}$$

For an induction motor with a shaft mounted cooling fan, the heat transfer coefficients are dependent on the rotor speed. This dependence has been modeled approximately by a set of linear relationships:

$$k_1 = k_{10}(1 + k_{1\omega}\omega_r) \tag{13}$$

$$k_2 = k_{20}(1 + k_{2\omega}\omega_r) \tag{14}$$

$$k_3 = k_{30}(1 + k_{3\omega}\omega_r) \tag{15}$$

Where: k_{10}, k_{20} and k_{30} thermal power transfer coefficients at the zero speed. k_{1w}, k_{2w} and k_{3w} variation of thermal power transfer with speed. Substitution into equations15 and 16 in the equations 13,14,17,18 and 19, and rearranging yields the thermal state equations for the stator and for the rotor [15]:

$$p\theta_s = \frac{R_s(\theta_s)}{H_s}(i_{ds}^2 + i_{qs}^2) + \frac{k_{ir}}{H_s}\omega_r^2 - \frac{k_{10}(1 + k_{1\omega}\omega_r)}{H_s}\theta_s + \frac{k_{30}(1 + k_{3\omega}\omega_r)}{H_s}(\theta_s - \theta_r) \tag{16}$$

$$p\theta_r = \frac{R_r(\theta_r)}{H_r}(i_{dr}^2 + i_{qr}^2) - \frac{k_{20}(1 + k_{2\omega}\omega_r)}{H_r}\theta_r + \frac{k_{30}(1 + k_{3\omega}\omega_r)}{H_r}(\theta_s - \theta_r) \tag{17}$$

The whole of preceding equations (6) a (9), (12), (20), and (21) us the model of following state:

$$p\delta i_{qr} = -L_1L_m\omega_r i_{ds} - R_s(\theta_s)L_2 i_{qs} - L_1L_2\omega_r i_{dr} + R_r(\theta_r)L_1 i_{qr} + L_m V_{qs} \tag{18}$$

$$p\delta i_{ds} = -R_s(\theta_s)L_2 i_{ds} + L_m^2\omega_r i_{qs} + R_r(\theta_r)L_m i_{dr} + L_2L_m\omega_r i_{qr} + L_2V_{ds} \tag{19}$$

$$p\delta i_{dr} = R_s(\theta_s)L_m i_{ds} - L_1L_m\omega_r i_{qs} - R_r(\theta_r)L_1 i_{dr} - L_1L_2\omega_r i_{qr} + L_2V_{qs} \tag{20}$$

$$p\delta i_{qs} = -L_m^2\omega_r i_{ds} - R_s(\theta_s)L_2 i_{qs} - L_2L_m\omega_r i_{dr} + R_r(\theta_r)L_m\omega_r i_{qr} + L_2V_{qs} \tag{21}$$

$$p\omega_r = p_nL_m(i_{qs}i_{dr} - i_{ds}i_{qr}) - \frac{b}{j}\omega_r + \frac{T_L}{j} \tag{22}$$

$$p\theta_s = \frac{R_s(\theta_s)}{H_s}(i_{ds}^2 + i_{qs}^2) + \frac{k_{ir}}{H_s}\omega_r^2 - \frac{k_{10}(1 + k_{1\omega}\omega_r)}{H_s}\theta_s + \frac{k_{30}(1 + k_{3\omega}\omega_r)}{H_s}(\theta_s - \theta_r) \tag{23}$$

$$p\theta_r = \frac{R_r(\theta_r)}{H_r}(i_{dr}^2 + i_{qr}^2) - \frac{k_{20}(1 + k_{2\omega}\omega_r)}{H_r}\theta_r + \frac{k_{30}(1 + k_{3\omega}\omega_r)}{H_r}(\theta_s - \theta_r) \tag{24}$$

This model has been tested and validated for several of operation of the induction motor, for more information the interested reader is invited to see [15].

ISSN 1737-9334

V. SIMULATION RESULTS

The main purpose of this simulation is to consider the influence of constant losses (hysteresis and eddy current) due to the frequency, the simulation results are illustrated in Figures 8 and 9. We note that the stator and rotor temperature at 60Hz is greater than the 50Hz.

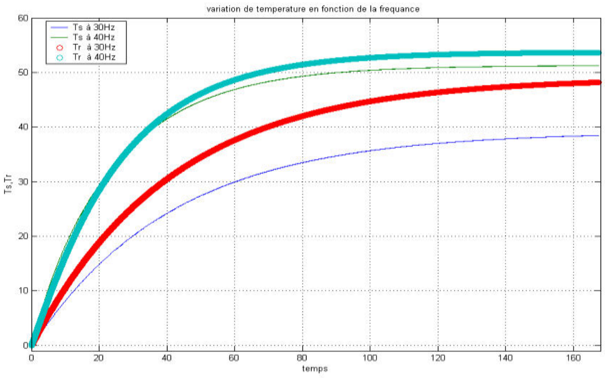

Fig. 8 stator and rotor temperature at 40 and 30 Hz

The stator and rotor temperature at 40Hz is greater than that at 30Hz.

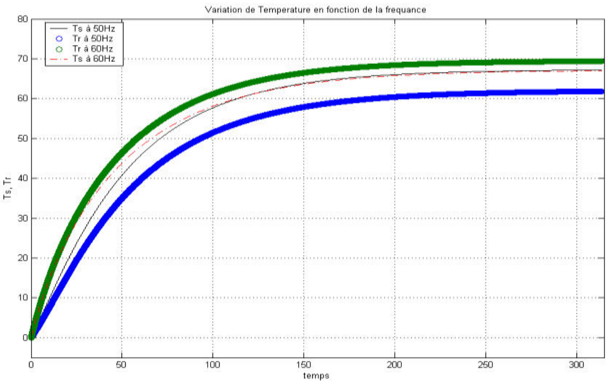

Fig. 9 stator and rotor temperature at -0 and 50 Hz

VI. CONCLUSION

In this paper, we presented a thermal model of a squirrel cage induction motor. This model is based on the theory of power dissipation, heat transfer and the rate of temperature increase in the rotor and stator, taking into account the effect of speed on the exchange. We summarize our results as that the temperature increase with the increasing of the frequency, this increasing is justified since the iron losses is a frequency depend and these losses transformed to heat.

ACKNOWLEDGEMENTS

This work was supported in part by Electrical Engineering Department, Department of Electrical Engineering, University of Chlef, UHBC, Algeria and in other part by Algerian ministry of research and High education.“

REFERENCE

[1] J. P. Bellomo, T. Lebey, F. Peltier and J. M. Oraison, “Conséquences des nouvelles formes de commande sur les matériaux de l'isolation statorique,” Journal de Physique III, vol. 7, pp. 993–1008, 1997.
[2] R. Glises, G. Hostache, and J. M. Kauffmann, “Simulation du comportement thermique en régime permanent d'un moteur asynchrone à refroidissement extérieur. Etude par éléments finis,” Journal de Physique III, vol. 4, pp. 1723–1735, 1994.
[3] H. Mellah, “Estimation des Grandeurs Intrinsèques d’une Machine Asynchrone,” 2018.
[4] E. Foulon, “Surveillance thermique de la machine asynchrone,” PhD thesis, Université de Nantes, 2005.
[5] L. Michalski, K. Eckersdorf, J. Kucharski and J. McGhee, Temperature Measurement, John Wiley & Sons, New York. 2002.
[6] H. Yahoui, and G. Grellet, “Measurement of physical signals in the rotating part of an electrical machine by means of optical fibre transmission, Measurement,” vol. 20, pp. 143–148, 1997.
[7] K. D. Hurst and T. G. Habetler, “A thermal monitoring and parameter tuning scheme for induction machines,” In IAS'97. Conference Record of the 1997 IEEE Industry Applications Conference Thirty-Second IAS Annual Meeting, vol. 1, pp. 136–142, 1997.
[8] M. Wegmuller, J. P. von der Weid, P. Oberson, and N. Gisin, “High resolution fiber distributed measurements with coherent OFDR,” in Proc. ECOC’00, 2000, paper 11.3.4, p. 109.
[9] E. Chauveau, E. H. Zaim, D. Trichet and J. Fouladgar, “A statistical approach of temperature calculation in electrical machines, IEEE T MAGN.,” vol. 36, pp. 1826–1829, 2000.
[10] S. B. Lee and T. G. Habetler, “An online stator winding resistance estimation technique for temperature monitoring of line-connected induction machines,” IEEE T IND APPL., vol. 39, pp. 685–694, 2003.
[11] Z. Lazarevic, R. Radosavljevic and P. Osmokrovic, “A novel approach for temperature estimation in squirrel-cage induction motor without sensors,” IEEE T INSTRUM MEAS.,” vol. 48, pp. 753–757, 1999.
[12] E. Chauveau, “Contribution au calcul électromagnétique et thermique des machines électriques - Application à l’étude de l’influence des harmoniques sur l’échauffement des moteurs asynchrones,” PhD thesis, Université de Nantes, 2001.
[13] H. Mellah and K.E. Hemsas, “The use of EKF to estimate the transient thermal behaviour of induction motor drive,” Journal of Electrical Engineering, vol. 1, pp. 40–47, 2013.
[14] E. Foulon, C. Forgez and L. Loron, “Resistances estimation with an extended Kalman filter in the objective of real-time thermal monitoring of the induction machine,” IET Electric Power Applications, vol. 1, pp. 549–556, 2007.
[15] J. K. Al-Tayie and P. P. Acarnley, “Estimation of speed, stator temperature and rotor temperature in cage induction motor drive using the extended Kalman filter algorithm,” IEE Proceedings-Electric Power Applications, vol. 144, pp. 301–309, 1997.
[16] H. Nestler and P. K. Sattler, “On-line-estimation of temperatures in electrical machines by an observer,” Electric machines and power systems, vol. 21, pp. 39–50, 1993.
[17] H. Mellah, K. E. Hemsas, R. Taleb and C. Cecati, “Estimation of speed, armature temperature, and resistance in brushed DC machines using a CFNN based on BFGS BP,” Turk J Elec Eng & Comp Sci., vol. 26, pp. 3181–3191, 2018.
[18] H. Mellah, K. E. Hemsas and R. Taleb, “Intelligent Sensor Based Bayesian Neural Network for Combined Parameters and States Estimation of a Brushed DC Motor,” International Journal of Advanced Computer Science and Applications-IJACSA, vol. 7, pp. 2530–235, 2016.
[19] H. Zhao, H. H. Eldeeb, J. Wang, Y. Zhan, G. Xu and O. A. Mohammed, “Online estimation of rotor temperature in induction motors based on parameter identification,” 2019 IEEE Energy Conversion Congress and Exposition (ECCE), Baltimore, MD, USA, pp. 1629-1634, 29 Sept.-3 Oct. 2019
[20] J. F. Moreno, F. P. Hidalgo and M. D. Martinez, “Realisation of tests to determine the parameters of the thermal model of an induction machine,” IEE Proceedings-Electric Power Applications, vol. 148, pp. 393–397, 2001.

ISSN 1737-9334

[21] T. Dong, X. Zhang, F. Zhou, and B. Zhao, "Correction of winding peak temperature detection in high frequency automotive electric machines," IEEE T Industrial Electronics, 2019.

[22] S. Xue, J. Feng, S. Guo, J. Peng, W. Q. Chu and Z. Q. Zhu, "A new iron loss model for temperature dependencies of hysteresis and eddy current losses in electrical machines," IEEE T MAGN., vol. 54, pp. 1-10, 2018.

[23] S. Xue, J. Feng, S. Guo, Z. Chen, J. Peng, W. Q. Chu and Z. Q. Zhu, "Iron loss model for electrical machine fed by low switching frequency inverter," IEEE T MAGN., vol. 53, pp. 1-4, 2017.

[24] R. Beguenane and M. E. H. Benbouzid, "Induction motors thermal monitoring by means of rotor resistance identification," IEEE T ENERGY CONVER., vol. 14, pp. 566–570, 1999.

[25] R. Beguenane and M. E. H. Benbouzid, "Induction motors thermal monitoring by means of rotor resistance identification," In 1997 IEEE International Electric Machines and Drives Conference Record, pp. TD2–4, 1997.

[26] H. Kubota, D. Yoshihara and K. Matsuse, "Rotor resistance adaptation for sensorless vector controlled induction machines," IEEJ Transactions on Industry Applications, vol. 117, pp. 940–945, 1997.

[27] S. B. Lee, T. G. Habetler, R. G. Harley and D. J. Gritter, "Stator and rotor resistance estimation technique for conductor temperature monitoring," In 35th IAS Annual Meeting and World Conference on Industrial Applications of Electrical Energy, pp. 381–387, 2000.

[28] M. S. N. Sdid and M. E. H. Benbouzid, "HG diagram based rotor parameters identification for induction motors thermal monitoring," IEEE T ENERGY CONVER., vol. 15, pp. 14–18; 2000.

[29] H. Mellah, K. E. Hemsas, A. Zorig and H. Radjeai, "Modélisation et surveillance thermique d'une machine asynchrone on prend on compte les effets no Linière," In International Conference on Power Electronics and Electrical Drives, ICPEED, 2010.

[30] A. T. Abdullah and A. M. Ali, "Thermal analysis of a three-phase induction motor based on motor-CAD, flux2D, and matlab," Indonesian Journal of Electrical Engineering and Computer Sciencem, vol. 15, pp. 46-53, 2019.
M. Schoning, E. Lange and K. Hameyer, "Development and validation of a fast thermal finite element solver," In 2008 18th International Conference on Electrical Machines, pp. 1–5, 2008.

[31] D. Sarkar, P. K. Mukherjee and S. K. Sen, "Use of 3-dimensional finite elements for computation of temperature distribution in the stator of an induction motor," In IEE Proceedings B, vol. 138, pp. 75–86, 1991.

[32] A. Boglietti, A. Cavagnino, D. Staton, M. Shanel, M. Mueller and C. Mejuto, "Evolution and modern approaches for thermal analysis of electrical machines," IEEE T IND ELECTRON, vol. 56, pp. 871–882, 2009.